Electronic Supplementary Information

Polyethylene Oxide-Based Solid-State Polymer Electrolyte Hybridized with Liquid Catholyte for Semi-Solid-State Rechargeable Mg-O_2 Batteries

Ayan Sarkar,[a] Shang-Yang Huang,[a] Vasantan Rasupillai Dharmaraj,[a,b] Behrouz Bazri,[a,c] Kevin Iputera,[a] Hsiu-Hui Su,[a] Yi-An Chen,[a] Han-Chen Chen,[d] Yu-Ping Lin,[d] Ren-Jei Chung,[*,b] Da-Hua Wei,[*,c] and Ru-Shi Liu[*,a]

[a] Department of Chemistry and the Advanced Research Center for Green Materials Science and Technology, National Taiwan University, Taipei 106, Taiwan.

[b] Department of Chemical Engineering and Biotechnology, National Taipei University of Technology (TAIPEI TECH), Taipei 106, Taiwan.

[c] Institute of Manufacturing Technology and Department of Mechanical Engineering, National Taipei University of Technology (TAIPEI TECH), Taipei 106, Taiwan.

[d] DEXIN Advanced Technology Co. Ltd., Zhubei City, Hsinchu County 302, Taiwan.

Corresponding Authors: R. J. Chung, Email ID: rjchung@ntut.edu.tw; D. H. Wei, Email ID: dhwei@ntut.edu.tw; R. S. Liu, Email ID: rsliu@ntu.edu.tw

Contents

1. Experimental Section

1.1. Materials and Reagents

The following materials/reagents were used: polyethylene oxide (PEO) ($[–CH_2CH_2O–]_n$, average molecular weight ($<M_W>$) ~600,000, Sigma–Aldrich), succinonitrile (SN) ($NCCH_2CH_2CN$, purity >99%, Thermo Scientific), magnesium triflate ($Mg(OTf)_2$) ($(CF_3SO_3)_2Mg$, purity 97%, Sigma–Aldrich), magnesium bis(trifluoro methanesulfonamide) ($Mg(TFSI)_2$, purity 99%, Sigma Aldrich), ruthenium (III) chloride hydrate ($RuCl_3 \cdot xH_2O$, 39% Ru content, UR Chemical Company Ltd.), multi-walled carbon nanotubes (MWCNT, <5% metal oxides, Sigma-Aldrich), poly(vinylidene fluoride) (PVDF) ($(CH_2CF_2)_n$, $<M_W>$ ~534000, Aldrich), anhydrous ethylene glycol (Sigma–Aldrich), acetonitrile (ACN) (CH_3CN, purity 99.9%, J. T. Baker), diglyme (G2) ($(CH_3OCH_2CH_2)_2O$, purity 99%, Alfa Aesar), anhydrous ethylene glycol (99.8% pure, Sigma–Aldrich), and N-methyl-2-pyrrolidone (NMP) (C_5H_9NO, >99% pure, Alfa Aesar).

1.2. Synthesis of PEO-$Mg(OTf)_2$ Polymer Electrolyte Membrane with [EO]: Mg^{2+} = 20: 1 with *x* wt.% SN

First, electrochemical impedance spectroscopy (EIS) results showed that among [EO]: Mg^{2+} = 10:1, 15:1, and 20:1, the 20:1 ratio gives the best room-temperature conductivity and good mechanical stability without stickiness.

About 5.5 mL of acetonitrile (ACN) was added dropwise to 0.44 g of PEO (<Mw> = 600,000) powder in a glass vial. ACN was selected because of its high dielectric constant (36.7), which is beneficial to better dissolve PEO and confer higher conductivity than methanol or acetone. A certain amount of SN (*x* wt.% of PEO's mass, *x* = 0–40%) was dissolved in 1.5 mL of ACN. After ~10 min, the solution was added dropwise to the PEO-ACN mixture. 2 mL of acetonitrile was used to dissolve 0.16122 g of $Mg(OTf)_2$ under stirring. After 4 h, the $Mg(OTf)_2$ solution was added (we noticed that this addition timing could influence the conductivity) to the PEO-SN solution, with excess ACN. The mixture was stirred for 18 h. If the polymer mixture is stirred for more hours, then the resulting polymer films show poor conductivity.

The solution was ultrasonicated to degas, poured into a Teflon Petri dish (inner diameter 3.8 cm), and left to dry at room temperature (RT) inside a humidity-controlled chamber. After 2 days of natural drying, the polymer membrane was dried inside the vacuum chamber of the

glove box. EIS studies showed that adding 30 wt.% SN offers the best conductivity; hence, 30% of 0.44 g (0.132 g SN) was added to PEO for the rest of the work. The prepared polymer with 30% SN has been named PEO-$Mg(OTf)_2$-30% SN. The average thickness of the polymer membrane was found to be ~0.30 mm.

1.3. Synthesis of Ru/CNT Cathode Catalyst

Ru/CNT nanomaterial was synthesized using the reflux method reported by our group previously.[1,2] About 50 mg of $RuCl_3 \cdot xH_2O$ and 80 mg of MWCNTs were poured into 100 mL of ethylene glycol in a round-bottom flask, and the mixture was ultra-sonicated for 40 min. The mixture was refluxed at 175 °C for 3 h under continuous magnetic stirring and nitrogen gas flow. After natural cooling, ethylene glycol was separated, and the black-colored residue was transferred to a Falcon tube. The black-colored sample was washed separately with ethanol (three times) and water (three times) in a centrifuge machine. Finally, the black sample was vacuum dried at 60 °C for 12 h, ground in a mortar pestle, and dried in the vacuum oven for 1 h to remove existing moisture. The ball-mill vessel was poured with 36 mg of Ru-CNT, 4 mg of PVDF, and 1 mL of NMP, and the vessel was subjected to ball-milling for 1 h at 3000 rpm to obtain a slurry.

1.3.1. Fabrication of Ru/CNT-CP cathode

Circular pieces of carbon paper (CP) were cut from a carbon paper sheet, cleaned with ethanol, and dried overnight in the vacuum oven. CP acts as the current collector and the gas diffusion layer. The slurry of Ru/CNT in NMP was ultrasonicated for 60 min and vortexed for 5 min before making the cathode. The circular pieces of the CP were weighed and noted in the microbalance. The ink-like Ru/CNT-NMP slurry was drop-casted and spread over the shiny surface of the circular CP pieces. The as-coated CP pieces were vacuum dried overnight at 60 °C to remove NMP and moisture. The vacuum-dried Ru-CNT-coated circular CP pieces were weighed again to determine the mass of the deposited Ru/CNT, which is the active cathode material. As Ru/CNT and PVDF were mixed in a 9:1 ratio, the active mass of Ru/CNT should be 90% of the total mass change of the carbon paper after coating Ru/CNT slurry and drying.

1.4. Coin Cell Assembly for Mg–O_2 Batteries

A CR2032-type coin cell was fabricated inside the Ar glove box (H_2O <0.1 ppm, O_2< 0.1 ppm). Ru/CNT-coated dried carbon paper (Ru/CNT-CP) was placed over the bottom case of the battery with a circular hole. A glass fiber (GF) separator was placed over the Ru/CNT-CP, and ~50–60 μL of 1 M $Mg(TFSI)_2$/G2 was added on the top of the glass fiber as the liquid

interphase. The freshly prepared PEO-$Mg(Tf)_2$-30%SN polymer electrolyte membrane was cut into a 10 mm-diameter disk with 0.30 mm thickness and placed over the GF. As PEO is soluble in G2, incorporating GF terminates the extensive dissolution of the PEO polymer membrane (in case of direct contact), thus protecting the cell from being short-circuited after some time. In addition, GF helps separate the Ru/CNT cathode after battery study for characterization. The polymer membrane adhered to the Ru/CNT cathode, making it inseparable for characterization. A well-polished and clean circular (8 mm diameter and 0.05 mm thickness) Mg (procured from Shinning Energy Company Ltd., Hsinchu, Taiwan) foil was used as the anode and placed over the electrolyte-coated separator. A spring was added on top of the Mg anode foil, and the upper battery cap was placed. Finally, the battery was sealed by pressing the machine. The cell assembly was prepared inside an MBraun Ar glovebox (O_2 < 0.1 ppm, H_2O < 0.1 ppm).

After the cell assembly, the cell was connected to the circuitry inside a 500 mL glass bottle. The glass bottle was purged with high-purity oxygen gas (2 N, 99%) for 10 min and then sealed.

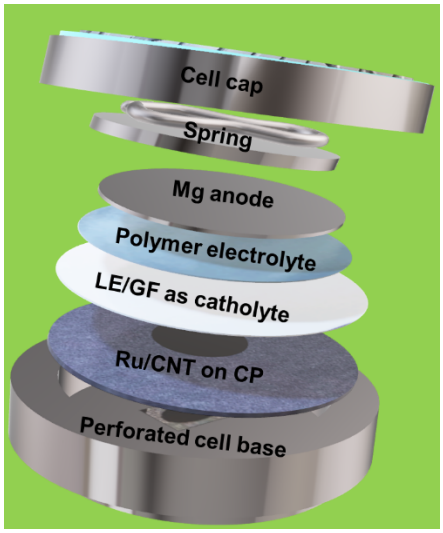

Figure S1. Coin cell architecture of the Mg–O_2 battery.

1.5. Pouch Cell Assembly

The polymer electrolyte-based pouch-type Mg–O_2 battery was assembled at the DEXIN Advanced Technology Co. Ltd. Aluminum-laminated film (ALF) was cut into 10 cm length and 6 cm width, with a square hole of 2 cm in length cut on one side after folding. A polypropylene (PP) plate was placed on the inner side of the uncut surface to facilitate electrode stacking. Mg metal pieces, with a side length of 2 cm, were inserted as anodes, and Ni tabs were affixed to the edges with polyimide (PI) tape for fixation. A 2 cm-long polymer electrolyte was inserted, followed by a 3 cm-long glass fiber separator, onto which 60 µL of 1 M

$Mg(TFSI)_2$ electrolyte was dropped. A 2 cm-long carbon paper cathode coated with CNT slurry was inserted, with Al tabs fixed to the edges of the carbon paper. This CNT slurry was processed similarly to Ru/CNT slurry processing, except that Ru NPs were not used (for cost management). After inserting the PP plate with a hole of 2 cm in side length to facilitate electrode compression, the four sides of the ALF were heat-sealed continuously for about 5 s at 180 °C by using a top sealing machine to complete the assembly of the pouch-typed Mg–O_2 battery.

1.6. Instrumentation

Electrochemical impedance spectroscopy (EIS) was conducted using a Metrohm Autolab electrochemical workstation (PGSTAT302N, AUT88379) with an ECI10M frequency booster module at 0 V with 10 mV_{rms} AC perturbation. Linear sweep voltammetry (LSV), cyclic voltammetry (CV), and amperometric *i-t* measurements were carried out using the same electrochemical workstation. The room-temperature galvanostatic discharge/charge cycles and maximum discharge capacity testing of the Mg–O_2 batteries were performed using an AccuTech Battery Testing System (BAT-750) from AccuTech Systems Co. Ltd. About 500 mAh g^{-1} curtailing capacity was sent for galvanostatic discharge–charge cycles. The time set for each discharge and charge process was 310 min. The voltage constraints for discharging and charging were set at 0.5 and 3.5 V, respectively.

Thermal gravimetry analysis (TGA) and differential thermal analysis were performed using a Rigaku STA8122 Thermo plus EVO2 series thermal analyzer in an argon gas environment. Room-temperature Raman spectroscopy was conducted using the Thermo Fisher DXRR Raman spectrometer equipped with a 532 nm laser light source. Fourier Transform Infrared (FTIR) spectra were recorded using a PerkinElmer's Spectrum Two FT-IR Spectrometer (L160000F) instrument in the attenuated total reflectance (ATR) method. Normal X-ray diffraction (XRD) patterns were recorded using a Bruker D2 phaser bench-top X-ray diffractometer by using Cu K_α line (λ = 1.5406 Å) as the X-ray source. Synchrotron XRD patterns of the pristine and discharged Ru/CNT cathodes were recorded at the National Synchrotron Radiation Research Center (NSRRC), Hsinchu City, Taiwan, and TLS 01C2 beamline with wavelength 0.77491 Å was used. X-ray absorption near edge structure (XANES) was also investigated at the NSRRC. X-ray photoelectron spectroscopy (XPS) was conducted using ULVAC-PHI's 5000 Versa Probe III model with monochromatic Al K_α X-ray source (1486.6 eV). Field emission electron microscopy (FESEM) studies were performed using the Zeiss Sigma electron microscope and JEOL JSM-7600F electron microscope equipped with an

OXFORD X-MaxN TSR energy-dispersive X-ray spectroscopy (EDS). JEOL JSM 6510 scanning electron microscope (SEM) was also used to take some relevant micrographs. JEOL JEM-2100F was used for transmission electron microscopy (TEM) and high-resolution transmission electron microscopy (HRTEM).

2. Supplementary Results and Discussion

2.1. Polymer Electrolyte Characterization

2.1.1. FWHM and XRD Peak Intensity

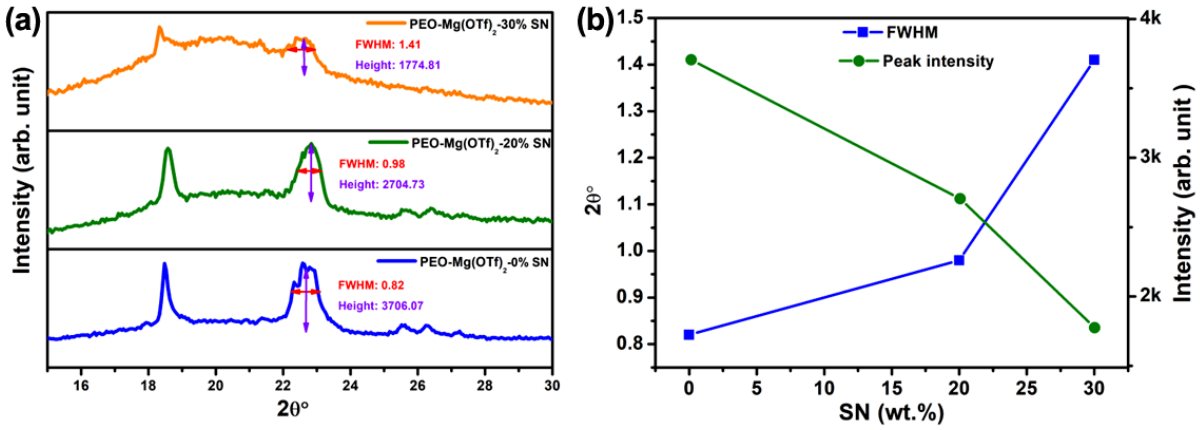

Figure S2. (a) Zoomed-in XRD patterns of PEO-Mg(OTf)$_2$-x% SN-based polymer electrolytes with x = 0, 20, and 30%. (b) Corresponding FWHM and peak intensity plots for the second XRD peak at ~22.58°.

2.1.2. Conductivity and Transference Number Calculations

Stainless steel|polymer electrolyte|stainless steel (SS)-based coin cell configuration has been used by EIS to measure the ionic conductivity of the polymer electrolytes.

The resistance (R) of a disk can be written as

$$R = \rho\frac{d}{\alpha}$$

$$\therefore \sigma = \frac{d}{R\alpha} \qquad \text{Equation S1}$$

Here, d is the thickness, and α is the area of the disk. ρ is the specific resistance; its reciprocal is called the conductivity (σ) tensor. The unit of σ is Ω^{-1} cm^{-1} or S cm^{-1}.

The bulk resistance of the electrolyte was estimated from the EIS study and used as the resistance for finding conductivity.

A RT Chronoamperometric study was conducted at 0.75 V to get the ionic transference number (t_{ion}) for the 30% SN-based polymer electrolyte (**Figure S3**(a)). The disk-shaped solid-state polymer electrolyte membrane was sandwiched between two stainless steel plates in a coin cell.

$$t_{ion} = 1 - \frac{I_e}{I_T} \qquad \text{Equation S2}$$

Here, I_e and I_T are the electronic and total currents, respectively. The RT t_{ion} for the polymer electrolyte is 0.997.

The electronic transference number t_e is given as I_e/I_T.

The total conductivity (σ_{total}) can be assumed as the sum of ionic conductivity (σ_{ion}) and electronic conductivity (σ_e),

$$t_e = \frac{I_e}{I_T} = \frac{\sigma_e}{\sigma_{total}} \qquad \text{Equation S3}^3$$

$$t_{ion} = \frac{\sigma_{ion}}{\sigma_{total}} \qquad \text{Equation S4}$$

$$\therefore\ \sigma_e = \sigma_{ion}\left(\frac{1}{t_{ion}} - 1\right) \qquad \text{Equation S5}$$

Taking $\sigma_{ion} = 39$ μS cm^{-1} and $t_{ion} = 0.997$, σ_e becomes 1.17 ×10^{-7} S cm^{-1}.

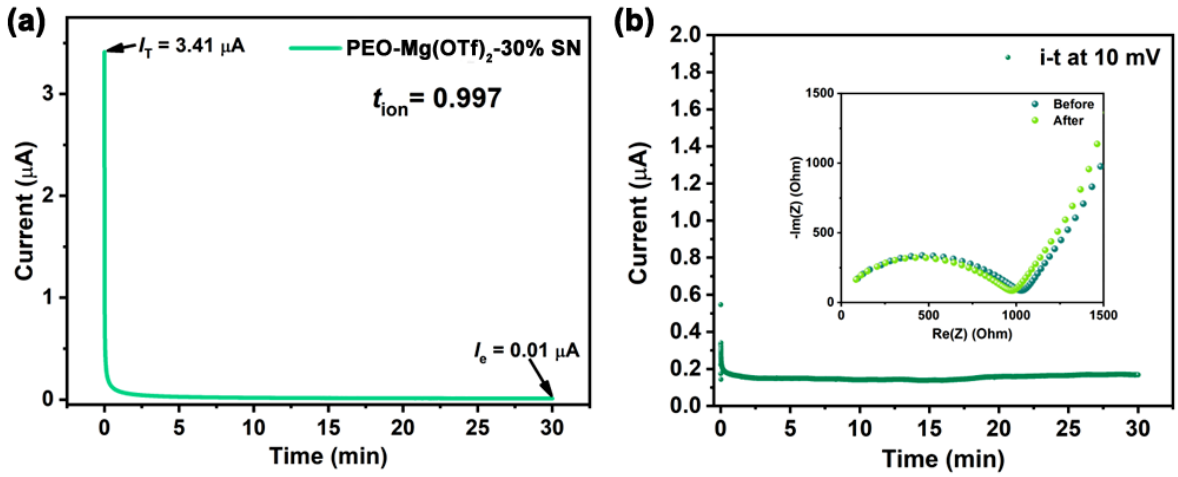

Figure S3. RT Amperometric *i-t* curves of PEO-Mg(OTf)$_2$-30% SN-based polymer electrolyte films at (a) 0.75 V with SS|polymer electrolyte|SS configuration and (b) 0.01 V with Mg|polymer electrolyte|Mg configuration.

The Mg ion transference number (t_{Mg}^{2+}) can be calculated using the following formula (Bruce-Vincent-Evans method).[4]

$$t_{Mg^{2+}} = \frac{I_{ss}(\Delta V - I_i R_i)}{I_i(\Delta V - I_{ss} R_{ss})} \qquad \text{Equation S6}$$

I_i and I_{ss} are the initial and steady-state currents, R_i and R_{ss} are the initial and steady-state resistances, respectively, and ΔV is the applied DC voltage polarization. **Figure S3**(b) depicts the Amperometric *i-t* curve recorded at 10 mV of a symmetric cell with Mg|polymer electrolyte|Mg configuration (coin cell). The t_{Mg}^{2+} value of the PEO-$Mg(OTf)_2$-30 wt.% SN-based polymer electrolyte has been found to be 0.29.

2.1.3. Morphology and Mechanical Properties of the PEO-$Mg(OTf)_2$-30% SN Polymer Electrolyte Membrane

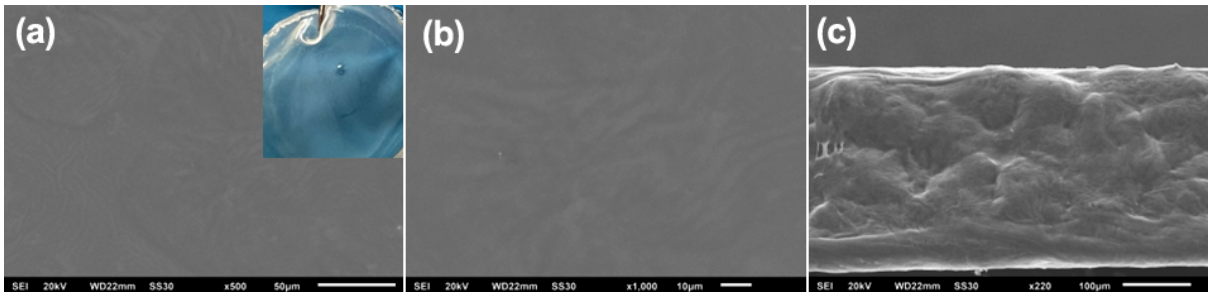

Figure S4. SEM micrographs of the PEO-$Mg(OTf)_2$-30% SN-based polymer membrane's surface at (a) lower magnification and (b) higher magnification. (c) Cross-sectional view of the polymer electrolyte. Inset of (a): digital photograph of a PEO-$Mg(OTf)_2$-30% SN-based polymer membrane with blue backdrop.

Figure S5. Maximum tensile stress measurement of the polymer electrolyte film.

Table S 1. Maximum tensile stress calculation.

Maximum Force (N)	Area (mm^2)	Maximum tensile stress (MPa)
0.307 kg × 9.81 m s^{-2} = 3.01 N	6	0.5017

2.1.4. Thermal Study

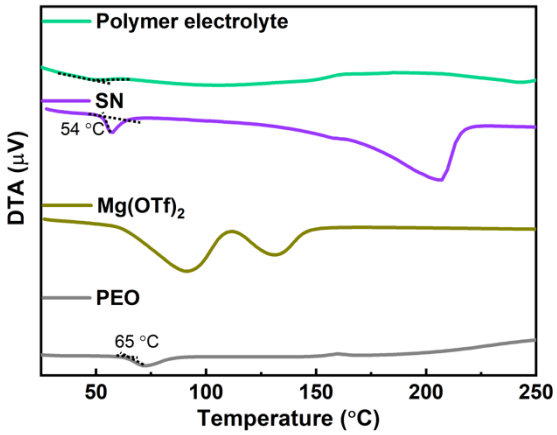

Figure S6. Differential thermal analysis (DTA) curves of PEO, $Mg(OTf)_2$, SN, and PEO-$Mg(OTf)_2$-30% SN polymer electrolyte up to 250 °C.

Figure S6 delineates the DTA curves of PEO, $Mg(OTf)_2$, SN, and PEO-$Mg(OTf)_2$-30% SN polymer electrolyte up to 250 °C. The melting temperature (T_m) has been estimated by finding the onset of the endothermic peak.

2.2. XPS of the Pristine Ru/CNT

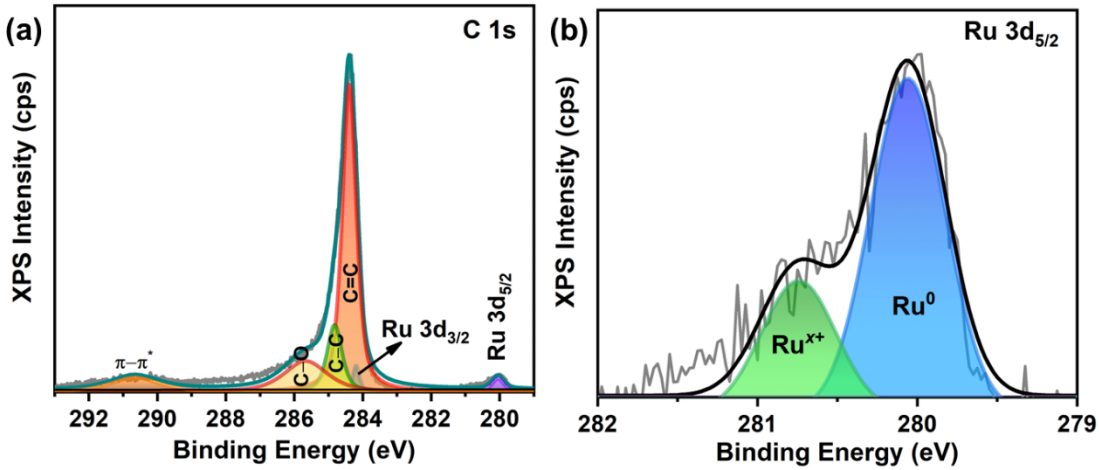

Figure S7. High-resolution curve-fitted XPS spectra of (a) C 1s and (b) Ru $3d_{5/2}$ for pristine Ru/CNT catalyst.

Figure S7(a) and (b) show the high-resolution Gaussian-Lorentzian curve-fitted XPS spectra of C 1s and Ru $3d_{5/2}$, respectively, of pristine Ru/CNT. All the data have been calibrated

against C 1s 284.8 eV peak. The intense C=C peak at 284.4 eV in the C 1s spectrum (**Figure S7**(a)) vividly shows a high amount of sp^2-hybridized carbon, which is beneficial to electronic conduction. Moreover, sp^3-hybridized C–C carbon (at 284.8 eV), C–O interaction (285.75 eV), and π–π* interactions (290.65 eV) can be verified from the C 1s XPS spectrum.[5,6] In the Ru $3d_{5/2}$ XPS spectrum (**Figure S7**(b)), partially oxidized Ru^{x+} states are present (280.75 eV) along with the metallic Ru^0 state (280.06 eV).[2] The partial oxidation of Ru occurs due to the air exposure of the Ru/CNT sample.[2] The simultaneous presence of sp^2-hybridized carbon and Ru^0 states synergistically help in catalysis for Mg–O_2 batteries.

2.3. Anode Comparisons for the Polymer Electrolyte-based and Liquid Electrolyte-based Mg–O_2 Cells

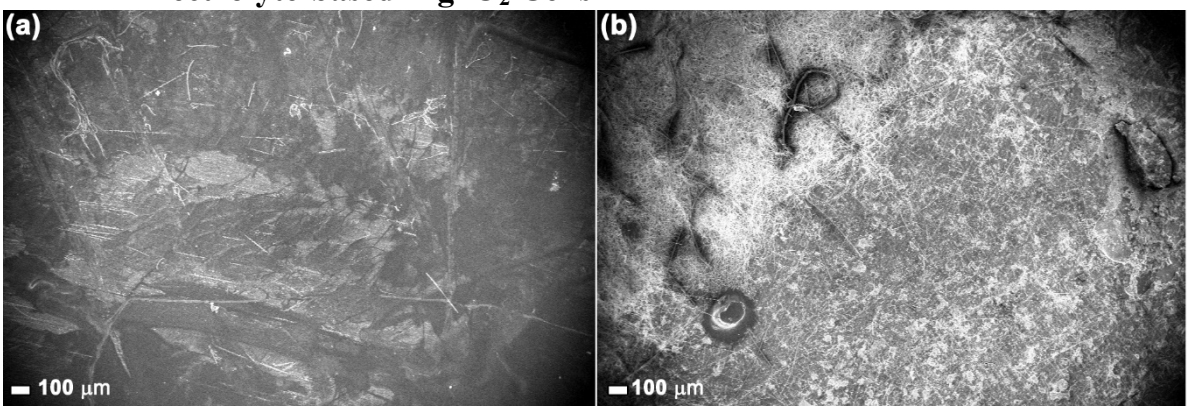

Figure S8. FESEM micrographs of the Mg anodes after maximum discharge of (a) polymer electrolyte-based and (b) 1 M $Mg(TFSI)_2$/G2 liquid electrolyte-based Mg–O_2 batteries taken under the same magnification.

2.4. GDC Cycling with 1 M $Mg(TFSI)_2$/G2

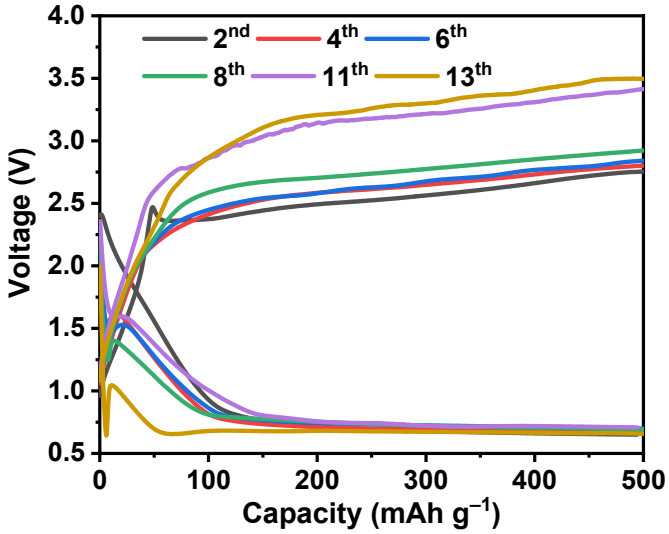

Figure S9. Galvanostatic discharge-charge cycles at 100 mA g^{-1} with 500 mAh g^{-1} cut-off capacity for an Mg–O_2 cell with 1 M $Mg(TFSI)_2$/G2 liquid electrolyte on glass fiber.

Figure S9 represents the galvanostatic discharge–charge cycling performance of an Mg–O_2 coin cell with 1 M $Mg(TFSI)_2$/G2 on glass fiber as the electrolyte. The amount of the liquid electrolyte was kept the same as the amount of 1 M $Mg(TFSI)_2$/G2 was added as the liquid interphase between the polymer electrolyte and Ru/CNT cathode catalyst. The battery could not perform well, and the cell could hardly run for 13 cycles with many inconsistencies and failures. The charging–discharging overpotential for the second cycle was 2.10 V, which increased to 2.84 V at the 13th cycle, substantiating a very poor battery performance of 50–60 µL of 1 M $Mg(TFSI)_2$ liquid electrolyte. Hence, adding this liquid electrolyte between the polymer electrolyte and Ru/CNT cathode catalyst helped establish a conducive liquid interphase between the solid-state polymer electrolyte and Ru/CNT, thereby facilitating ion transfer and gas dissolution.

2.5. Discharged Ru/CNT Cathode Characterization

2.5.1. Synchrotron XRD Patterns

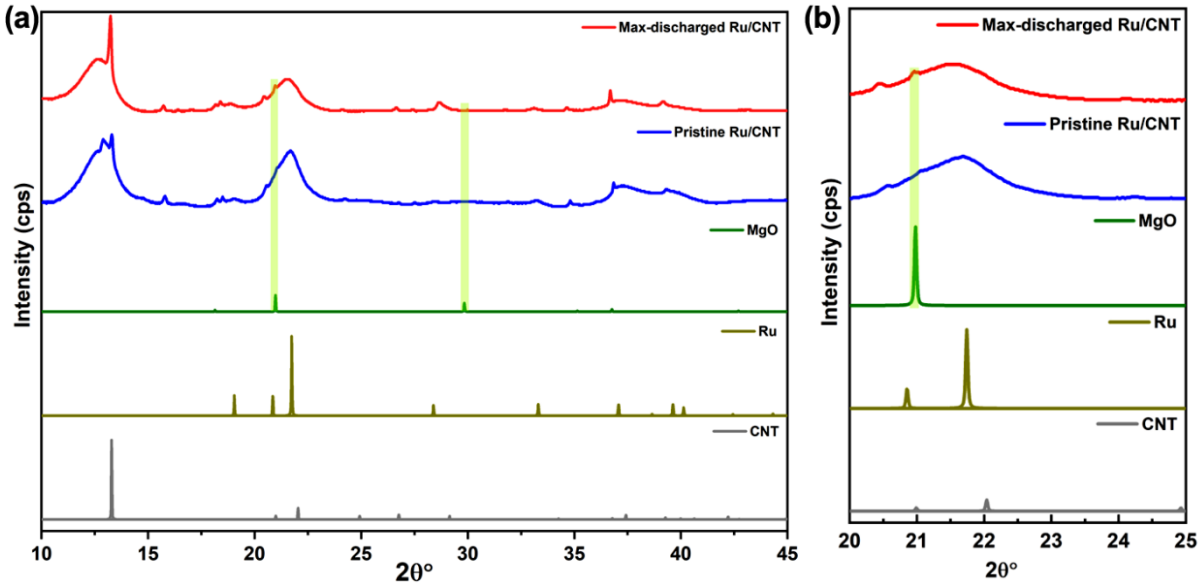

Figure S10. (a) Synchrotron XRD patterns of the pristine Ru/CNT cathode and maximum discharged Ru/CNT cathode. Ru, CNT, and MgO reference patterns have been generated using VESTA. (b) Zoomed-in view of the XRD patterns in the 20°–25° range.

Figure S10 shows the synchrotron XRD (wavelength of the photon beam is 0.77491 Å) patterns of the pristine Ru/CNT and maximum discharged Ru/CNT cathodes. Based on a comparison of the synchrotron XRD patterns, the presence of MgO can be verified as the discharge product for the Mg–O_2 battery with the prominent peak at 20.963°, indicating the $(0\ \bar{2}0)$ plane of MgO.

2.5.2. FESEM Micrographs

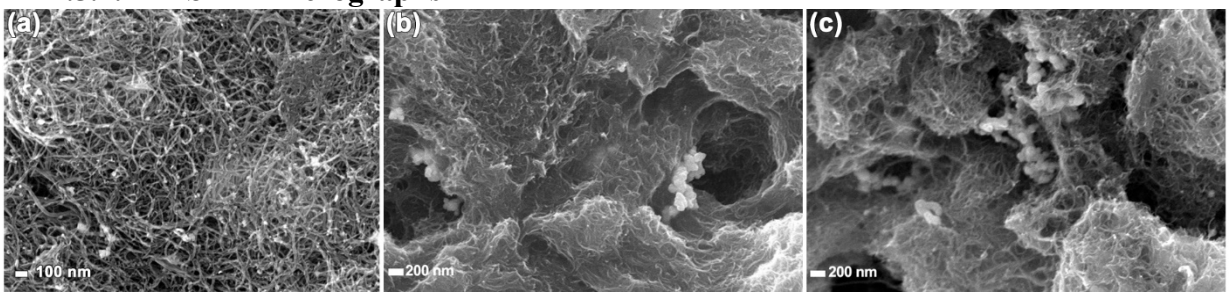

Figure S11. FESEM micrographs of the Ru/CNT cathodes (a) at pristine conditions, (b) after the first GDC discharge cycle, and (b) after the first GDC charge cycle.

2.5.3. Raman Spectroscopy

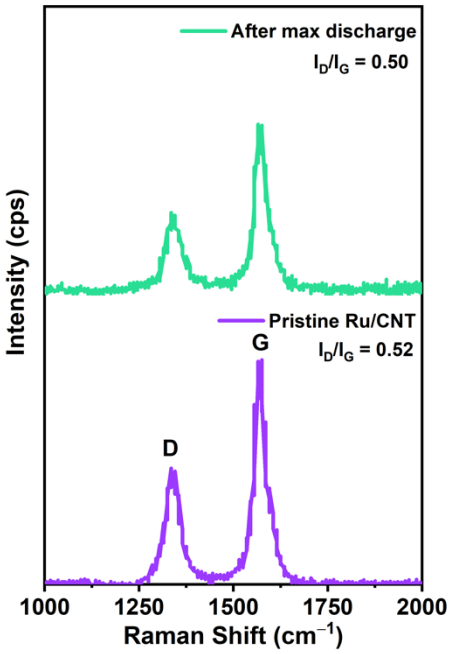

Figure S12. Raman spectra of the pristine Ru/CNT cathode and the Ru/CNT cathode after the maximum discharge.

The Raman spectra of the pristine Ru/CNT cathode and the Ru/CNT cathode after the maximum discharge are portrayed in **Figure S12**. Each spectrum comprises two bands, namely, D and G. The D and G bands are positioned at 1338.1 and 1568.0 cm^{-1}, respectively, for pristine Ru/CNT. The D and G bands are centered at 1340.30 and 1570.23 cm^{-1}, respectively, for the maximum discharged cathode. The intensities of the D and G bands are denoted as I_D and I_G, respectively. The I_D: I_G ratio for pristine Ru/CNT was 0.52; however, the I_D: I_G ratio remained almost the same after maximum discharge (0.50), suggesting that the Ru/CNT cathode was not chemically damaged after the maximum discharge.

2.6. Catholyte-related Studies

2.6.1. Raman Spectroscopy and EIS

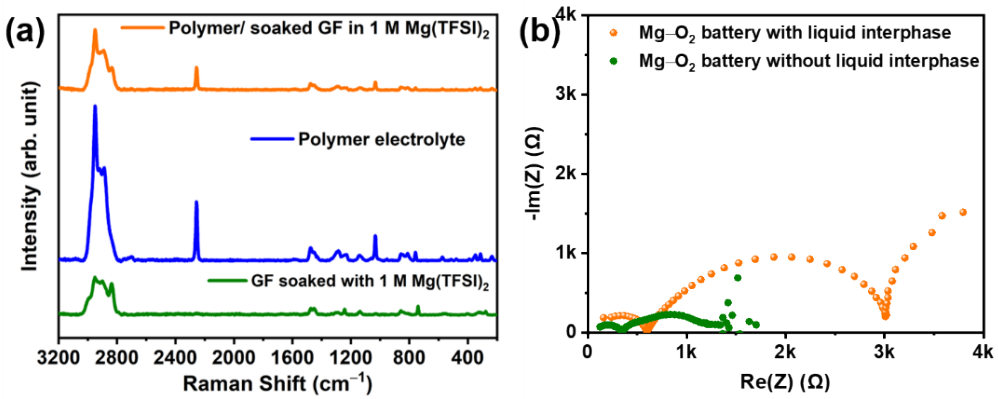

Figure S13. (a) Raman spectra of GF soaked in 1 M $Mg(TFSI)_2$/G2, polymer electrolyte membrane, and the polymer membrane after touching its surface with a glass fiber soaked with 50 µL of 1 M $Mg(TFSI)_2$/G2 for some time. (b) Nyquist plots of Mg–O_2 batteries with and without catholytes.

2.6.2. $Mg(OTf)_2$/G2-based Catholyte

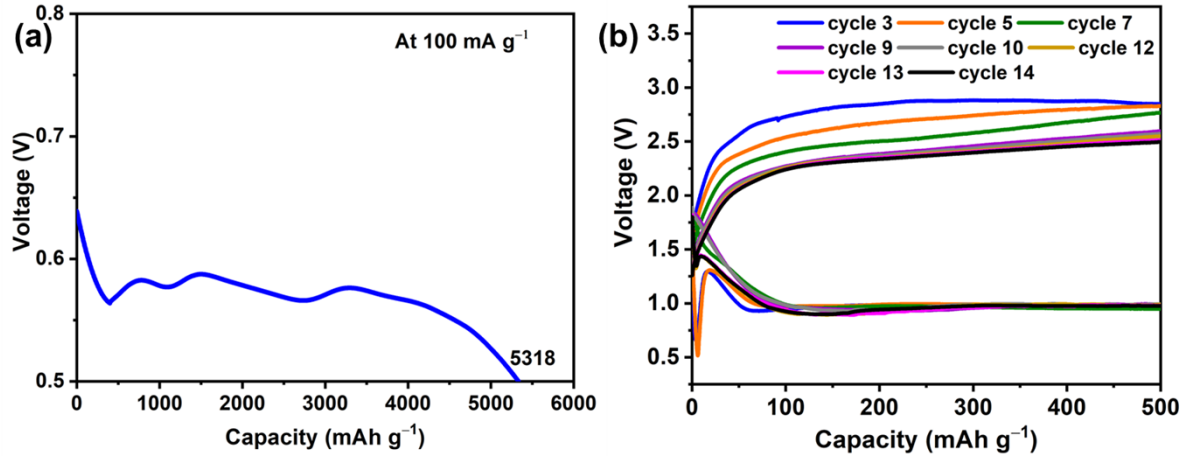

Figure S14. (a) Galvanostatic maximum discharge capacity at 100 mA g^{-1} and (b) galvanostatic discharge–charge cycling performance at 100 mA g^{-1} for Mg–O_2 coin cell batteries with $Mg(OTf)_2$/G2-based liquid catholyte.

When the $Mg(OTf)_2$/G2-based catholyte was used instead of the $Mg(TFSI)_2$/G2-based catholyte, the Mg–O_2 battery performance was not impressive. In particular, 1 M $Mg(OTf)_2$ could not be dissolved in diglyme, and 0.5 M $Mg(OTf)_2$ was proven inferior to 1 M $Mg(TFSI)_2$ in terms of battery performance.

The battery produced 5318 mAh g^{-1} deep discharge capacity at 100 mA g^{-1} and ran for unsteady 14 cycles with higher charging–discharging overpotential (**Figure S14**). The open circuit

potential was substantially low, and the deep discharge curve was wavy for the $Mg(OTf)_2$/G2 catholyte-based Mg–O_2 batteries, as shown in **Figure S14**(a).

2.7. EIS of the Full Cell at Open Circuit Potential: Before and During Cycling

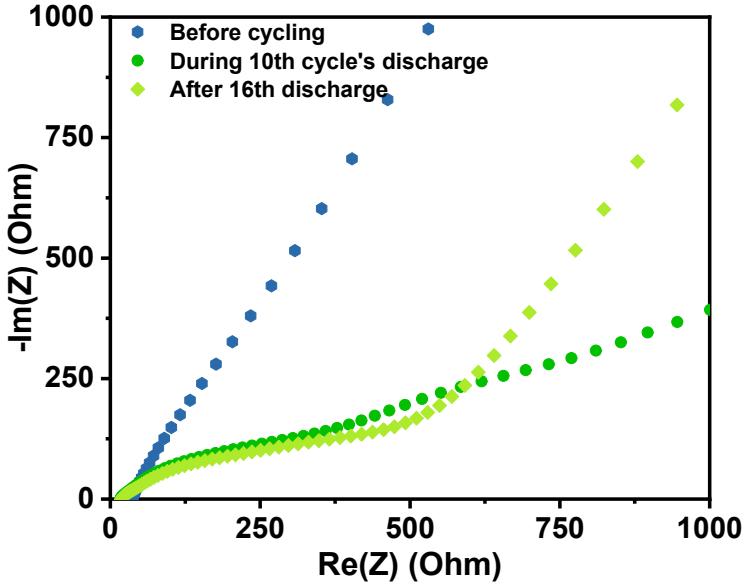

Figure S15. Nyquist plots of a Mg-O_2 full cell taken by recording RT EIS at open circuit potentials (OCP) before cycling, during the 10th discharge, and after the 16th discharge at 100 mA g^{-1}.

RT EIS measurements were carried out at OCPs of a Mg–O_2 full cell before and during cycling. **Figure S15** represents the corresponding Nyquist plots, from which it can be seen that the bulk resistance slightly improved on cycling. The total resistance, which includes interphase and charge transfer resistances, improved slightly after the 16th cycle (1504 Ohm) than the 10th cycle (1654 Ohm), which could be attributed to the formation of a conducive MgF_2-rich interphase layer at the Mg anode side.

References

1 K. V. Savunthari, C. H. Chen, Y. R. Chen, Z. Tong, K. Iputera, F. M. Wang, C. C. Hsu, D. H. Wei, S. F. Hu and R. S. Liu, *ACS Appl. Mater. Interfaces*, 2021, **13**, 44266–44273.

2 V. Rasupillai Dharmaraj, A. Sarkar, C. H. Yi, K. Iputera, S. Y. Huang, R. J. Chung, S. F. Hu and R. S. Liu, *ACS Appl. Mater. Interfaces*, 2023, **15**, 9675–9684.

3 Z. Osman, M. I. Mohd Ghazali, L. Othman and K. B. Md Isa, *Results Phys.*, 2012, **2**, 1–4.

4 J. Evans, C. A. Vincent and P. G. Bruce, *Polymer (Guildf).*, 1987, **28**, 2324–2328.

5 M. C. Biesinger, *Appl. Surf. Sci.*, 2022, **597**, 153681.

6 A. Sarkar, K. Karmakar, A. K. Singh, K. Mandal and G. G. Khan, *Phys. Chem. Chem. Phys.*, 2016, **18**, 26900–26912.